

Preparation and electrochemical properties of perovskite $\text{Ce}_x\text{Li}_{0.5-x}\text{Ca}_{0.5}\text{TiO}_3$ composites

J H Cheng¹, C A Tian

Department of Chemistry and Materials Engineering, Hefei University, Hefei, 230601 Anhui, China

¹E-mail: cjh@hfu.edu.cn

Abstract. Composites with perovskite structure based on lithium and cerium co-doped CaTiO_3 , $\text{Ce}_x\text{Li}_{0.5-x}\text{Ca}_{0.5}\text{TiO}_3$ was prepared by the sol-gel method. Phase structure and morphology of the powders were carried out by X-ray diffraction (XRD) and transmission electron microscopy (TEM). The results show that the $\text{Ce}_x\text{Li}_{0.5-x}\text{Ca}_{0.5}\text{TiO}_3$ powders have cubic perovskite structures after sintered above 800 °C and the mean size of the $\text{Ce}_x\text{Li}_{0.5-x}\text{Ca}_{0.5}\text{TiO}_3$ powders is about 60 nm. A study of ionic conductivity by electrochemical impedance spectroscopy (EIS) implies that the conductivity of $\text{Ce}_x\text{Li}_{0.5-x}\text{Ca}_{0.5}\text{TiO}_3$ increases with the increasing of the contents of Ce^{3+} dopant and reaches a maximum value of $2.1 \times 10^{-4} \text{ S} \cdot \text{cm}^{-1}$ at $x = 0.05$, and then decreases for $x > 0.05$.

1. Introduction

Solid electrolyte is a key component of solid-state electrochemical devices, which are widely applied in energy conversion, chemical processing, sensing, and combustion control [1-4]. For most of these applications, high ionic conductivity of the solid electrolyte is required for device performance, and more and more studies have been carried out for the improvement of its ionic conductivity [5].

The perovskite structure is one of the most wonderful to exist in nature. At present, the application of perovskite structure composites is applied largely because of their superior conductivities, and the influence of various additives on the electrical properties of calcium, strontium and barium titanate has been widely investigated [6-9]. CaTiO_3 is ABO_3 type perovskite structure, it is cubic crystal system at high temperature. In cubic system, the doping of metal cations with different valences can induce the distortions of oxygen stoichiometric ratio and crystal lattice to form nonstoichiometric compounds easily. High-temperature electrical conductivity of undoped CaTiO_3 were studied by W.L. George [10]. According to this research the defect structure of calcium titanate at high temperatures maybe described by majority defect pairs of oxygen vacancies and excess electrons. More recently, several studies on doped calcium titanates were reported [11-14]. Among all doped CaTiO_3 materials, lithium doped CaTiO_3 composite has a higher conductivity at low temperatures, and has attracted much attention in recent years [15-18].

Lithium doped CaTiO_3 , $\text{Li}_x\text{Ca}_{1-x}\text{TiO}_3$ have been prepared in our previous studies [19]. The object of the present work was to study the preparation and characterization of $\text{Ce}_x\text{Li}_{0.5-x}\text{Ca}_{0.5}\text{TiO}_3$ composites. Solid solutions $\text{Ce}_x\text{Li}_{0.5-x}\text{Ca}_{0.5}\text{TiO}_3$ were synthesized by a sol-gel method in this study, and the phase constitution and shape of the powders were characterized by X-ray diffraction and transmission electron microscopy, ionic conductivity of the pellets was investigated through AC impedance.



2. Experimental

$Ce_xLi_{0.5-x}Ca_{0.5}TiO_3$ powders were prepared by a sol-gel method in the present study. All the raw materials were purchased from Sinopharm Chemical Reagent Co., Ltd., China. In this process, $Ti(OC_4H_9)_4$ and acetylacetonate were dissolved in absolute alcohol (volume ratio of employed $Ti(OC_4H_9)_4$, absolute alcohol and acetylacetonate was 4:4:1) by stirring and heating at 40°C, then the mixture, which formed by $Ca(NO_3)_2 \cdot 4H_2O$, $LiNO_3$ and $Ce(NO_3)_3 \cdot 6H_2O$ dissolved in deionized water, were added into the solution drop by drop under constant stirring. After the precursor solution reacted at 40 °C for 4 h, the $Ce_xLi_{0.5-x}Ca_{0.5}TiO_3$ sol was obtained. Subsequently, the sol was kept in an oven at 50 °C for 48 h to get the dried gel. Then the dried gel was calcined in air at 600 °C, 700 °C and 800 °C for 2 h respectively, the needed powders were obtained. The powders were then pressed into discs of 12 mm in diameter and 1 mm in thickness at a pressure of 30 MPa. At last, the green discs are sintered in a high-temperature furnace at 1400 °C for 6 h to form the ceramic discs. To measure the ionic conductivity of the samples, the silver paste conductive adhesive was coated on both surfaces of the calcined pellets.

X-ray diffraction (XRD) analysis was measured with a Japanese D/max- γ B rotating diffractometer, and the diffractograms were scanned in 2θ from 10° to 70° at a rate of 6° min⁻¹. Transmission electron microscopy (TEM) photographs were taken on a JEM-100SX transmission electron microscope. The measurement of electrochemical impedance (EIS) was performed with an electrochemical workstation CHI660B at a frequency range of 1 Hz to 100 kHz at room temperature in air.

3. Results and discussion

3.1. Phase of $Ce_xLi_{0.5-x}Ca_{0.5}TiO_3$

The X-ray diffraction patterns of $Ce_{0.05}Li_{0.45}Ca_{0.5}TiO_3$ powders sintered at different temperatures are shown in figure 1. The patterns were indexed on the basis of a distorted perovskite structure with cubic symmetry (space group $Fd\bar{3}m$). Figure 1 is the XRD patterns of $Ce_{0.05}Li_{0.45}Ca_{0.5}TiO_3$ powders sintered at different temperatures. Although the typical diffraction peaks of cubic perovskite structure occurred at 600 °C, but the intensity of the diffraction peaks were weak, and some characteristic peaks were not observed, which indicate that the sample was not well crystallized at this temperature. When the sintering temperature increased to 800 °C, the appearance of typical diffraction peaks indicated that the powders have crystallized well and formed cubic perovskite structure with space group $Fd\bar{3}m$. The typical three diffraction lines ((111), (200), and (311) reflections) are assigned, suggesting that the $Ce_{0.05}Li_{0.45}Ca_{0.5}TiO_3$ powders have a cubic perovskite structure and the $Ce_{0.05}Li_{0.45}Ca_{0.5}TiO_3$ powders conduct the transition from amorphous to crystalline at 600 °C-800 °C.

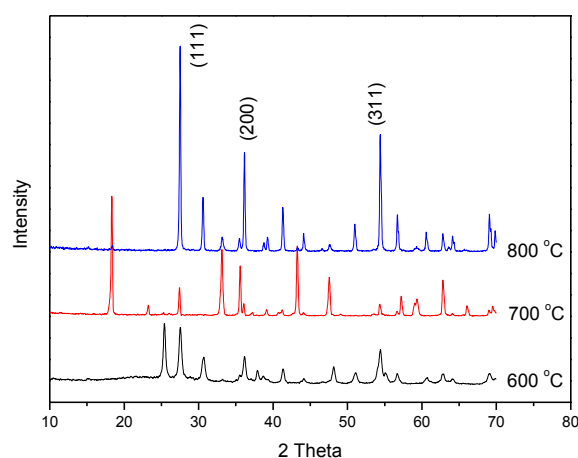


Figure 1. X-ray diffraction patterns of $Ce_{0.05}Li_{0.45}Ca_{0.5}TiO_3$ powders treated at different temperatures.

The mean size of the prepared powders was calculated to be about 60nm based on Scherrer formula.

$$D=0.89\lambda/B\cos\theta \quad (1)$$

Where λ is the wavelength of X-ray (Cu $K\alpha$ radiation, $\lambda=0.154056$ nm), θ is the diffraction angle, $B=\sqrt{Bm^2 - Bs^2}$ is the corrected halfwidth of the observed halfwidth: Bm is that of the (111) reflection in samples and Bs is that of the (111) reflection in a standard sample.

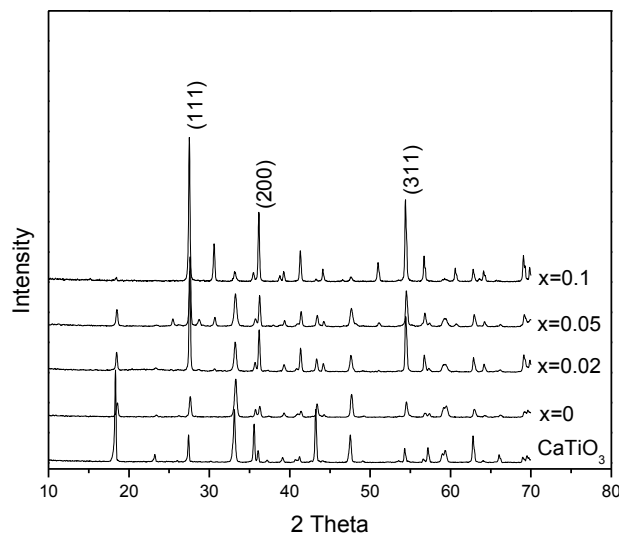


Figure 2. X-ray diffraction patterns of $Ce_xLi_{0.5-x}Ca_{0.5}TiO_3$ ($x=0\sim 0.1$) sintered at 800 °C.

Figure 2 is the X-ray diffraction patterns of $Ce_xLi_{0.5-x}Ca_{0.5}TiO_3$ with different content x prepared by the sol-gel synthesis. As seen from the figure, all these XRD patterns are similar to that of $CaTiO_3$, and there is no evident secondary phases or superstructure could be identified. The result indicates that a relatively low calcinations temperature is satisfiable to prepare pure phase of $Ce_xLi_{0.5-x}Ca_{0.5}TiO_3$ powders with perovskite structure. When $CaTiO_3$ doped with Li and Ce, Ca^{2+} were substituted by Li^+ and Ce^{3+} ions partially formed $Ce_xLi_{0.5-x}Ca_{0.5}TiO_3$ solution. But the amount of Li^+ and Ce^{3+} ions is not more, so this change is not strong enough to distort the $CaTiO_3$ structure, and $Ce_xLi_{0.5-x}Ca_{0.5}TiO_3$ remains cubic perovskite structure alike $CaTiO_3$ [20].

3.2. Morphology of $Ce_{0.05}Li_{0.45}Ca_{0.5}TiO_3$

Figure 3 is the TEM photographs of $Ce_{0.05}Li_{0.45}Ca_{0.5}TiO_3$ powders calcined at different temperatures. The $Ce_{0.05}Li_{0.45}Ca_{0.5}TiO_3$ powders calcined at 600 °C are agglomerated in lump, moreover, the shape of each grain is irregular and the grain boundary is obscure (shown as figure 3a). But when calcining temperature reached at 800 °C, the powders are mono-dispersed and the mean grain size is about 60 nm shown as figure 3b. These results indicate that the $Ce_{0.05}Li_{0.45}Ca_{0.5}TiO_3$ powders are amorphous at 600 °C, but have crystallized well at 800 °C, and the particle size of the powders with a narrow particle size distribution is small and increases with the increase of the calcining temperature. This fact agrees the conclusion drawn from XRD analysis.

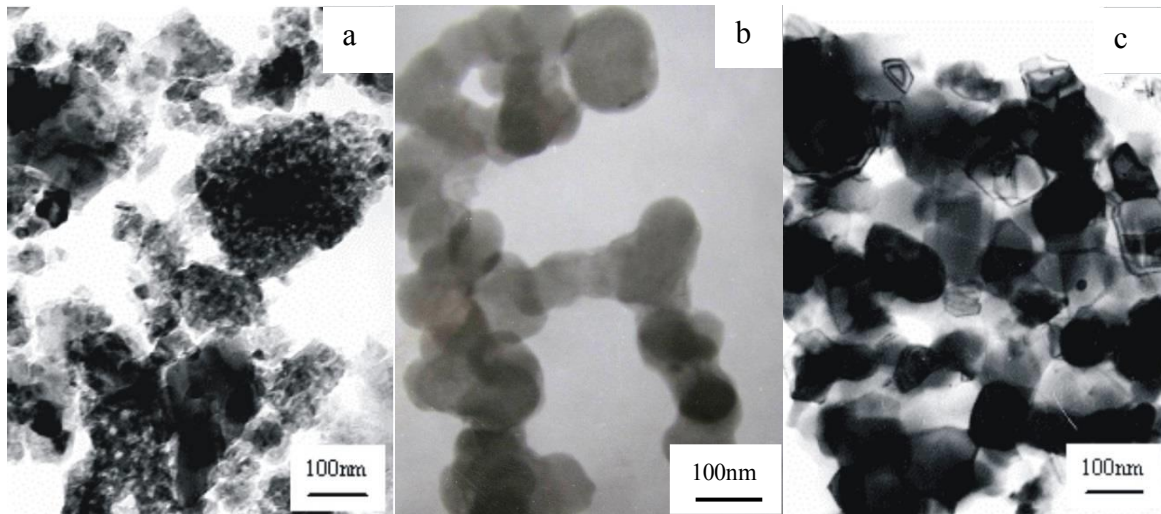


Figure 3. TEM photographs of $\text{Ce}_{0.05}\text{Li}_{0.45}\text{Ca}_{0.5}\text{TiO}_3$ powders calcined at 600 °C (a), 700 °C (b) and 800 °C (c).

3.3. Sinterability analysis

The bulk density (ρ) of sintered pellets was calculated using Archimedes' method in deionized water (D.I. water):

$$\rho = \frac{W_{Dry} \times \rho_{Water}}{W_{Wet} - W_{Sus}} \quad (2)$$

where W_{Dry} is the dry weight of sintered discs, ρ_{water} is the density of D.I. water ($0.997 \text{ g}\cdot\text{cm}^{-3}$), W_{Wet} represents the wet weight (put the pellet in water and boiling for 30 min), and W_{sus} shows the suspended weight of sintered discs in D.I. water. The values of the relative densities reached above 95% when sintering temperature was 1400 °C, which resulted in the formation of dense discs with low porosity.

3.4. Ionic conductivity of $\text{Ce}_x\text{Li}_{0.5-x}\text{Ca}_{0.5}\text{TiO}_3$

An interesting approach to the study of the electrical behavior of compounds is the electrochemical impedance spectroscopy (EIS) technique [21]. Figure 4 is the electrochemical impedance spectra of $\text{Ce}_x\text{Li}_{0.5-x}\text{Ca}_{0.5}\text{TiO}_3$ pellets sintered at 1400 °C. Each spectrum consists of an incomplete semicircle and an inclined line shown as figure 4. In principle, a semicircle between the origin and the intercept would be observed if much higher frequency were used in the experiment, but the high-frequency limit used in this study (100 kHz is the upper limit for electrochemical workstation CHI660B) is not sufficient and caused the incomplete semicircle [22].

The replacement of A or B-metal in a ABO_3 perovskite by a cation of lower valence, oxygen vacancies are formed, whose concentration is equal to the defects. Conductivity dependence on oxygen partial pressure may be divided into two areas: in the intermediate oxygen partial pressure area where CaTiO_3 conductivity is proportional to $p^{1/6}\text{O}_2$, and the low partial pressures area, where the obtained experimental dependences increase [23, 24].

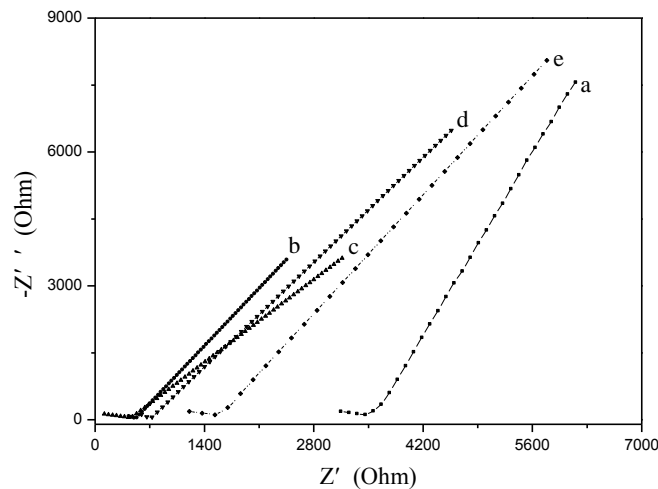


Figure 4. AC impedance curves of pellets, (a) $x=0$, (b) $x=0.02$, (c) $x=0.05$, (d) $x=0.1$, (e) $x=0.2$.

The intercepts of the semicircular arcs at “z” axes provide the resistance values corresponding to bulk (R_{gi}) and grain boundaries (R_{gb}). The conductivities can be calculated using the resistance obtained by fitting the impedance spectra using ZSimpWin software. Then the conductivity datums at different temperatures can be obtained using the equation (3). The ionic conductivities of the $\text{Li}_{0.5}\text{Ca}_{0.5}\text{TiO}_3$, $\text{Ce}_{0.02}\text{Li}_{0.48}\text{Ca}_{0.5}\text{TiO}_3$, $\text{Ce}_{0.05}\text{Li}_{0.45}\text{Ca}_{0.5}\text{TiO}_3$, $\text{Ce}_{0.1}\text{Li}_{0.4}\text{Ca}_{0.5}\text{TiO}_3$ and $\text{Ce}_{0.2}\text{Li}_{0.3}\text{Ca}_{0.5}\text{TiO}_3$ samples prepared by sol-gel technique at room temperature can be estimated to be $8.66 \times 10^{-5} \text{ S}\cdot\text{cm}^{-1}$, $1.63 \times 10^{-4} \text{ S}\cdot\text{cm}^{-1}$, $2.1 \times 10^{-4} \text{ S}\cdot\text{cm}^{-1}$, $1.9 \times 10^{-4} \text{ S}\cdot\text{cm}^{-1}$ and $9.81 \times 10^{-5} \text{ S}\cdot\text{cm}^{-1}$ respectively. These values are near to that of other fluorite type electrolytes such as YSZ, SDC or GDC which have been studied in-depth for SOFCs applications.

$$\sigma = L/R \cdot S \quad (3)$$

Where L and S is the thickness and the area of the pellet, respectively. R is the resistance of the sample (The resistances $R=R_{gi}+R_{gb}$). These datum indicate that the $\text{Ce}_x\text{Li}_{0.5-x}\text{Ca}_{0.5}\text{TiO}_3$ ionic conductivity increases with the increasing of the contents of Ce^{3+} dopant and reaches a maximum value at $x=0.05$, and then decreases for $x > 0.05$. When the oxygen vacancies were substituted by Li^+ and Ce^{3+} ions, the ionic conductivities of $\text{Ce}_x\text{Li}_{0.5-x}\text{Ca}_{0.5}\text{TiO}_3$ solid solutions were significantly improved, but when the amount of the substituted Li^+ and Ce^{3+} ions exceeded a certain value, the interactions among dopant cations (Li^+ and Ce^{3+}) and higher concentrations of oxygen vacancies caused the aggregating of oxygen vacancies, so the effective oxygen vacancies concentration did not increase and the ionic conductivity was lowering for $x > 0.05$.

4. Conclusions

The perovskite structure solution with chemical formula of $\text{Ce}_x\text{Li}_{0.5-x}\text{Ca}_{0.5}\text{TiO}_3$ were prepared by the sol-gel method in ethanol and water mixture medium. The products formed pure cubic perovskite structure after calcined at 800°C , and the mean size of the $\text{Ce}_x\text{Li}_{0.5-x}\text{Ca}_{0.5}\text{TiO}_3$ powders calculated to be about 60 nm. The ionic conductivity at room temperature of $\text{Ce}_x\text{Li}_{0.5-x}\text{Ca}_{0.5}\text{TiO}_3$ increases with the increase of the contents of Ce^{3+} dopant and reaches a maximum value of $2.1 \times 10^{-4} \text{ S}\cdot\text{cm}^{-1}$ at $x=0.05$, and then decreases for $x > 0.05$.

Acknowledgements

Research supported by the Natural Science Foundation of Education Department of Anhui Province under contract No. KJ2016A591, the Nature Science Foundation of Anhui Province of China under contract No. 1708085ME112 and the Key projects of Foreign visits to key Teachers of Universities in Anhui Province under contract No. gxfxZD2016220.

References

- [1] Ishihara T, Matsuda H, Azmi Bin Bustam M and Takita Y 1996 *Solid State Ionics* **86-88** 197
- [2] Xie K, Yan R, Chen X, Dong D, Wang S, Liu X and Meng G 2009 *J. Alloys Compd.* **472** 551
- [3] Liou Y and Yang S 2008 *J. Power Sources* **179** 553
- [4] Li S, Li Z and Bergman B 2010 *J. Alloys Compd.* **492** 392
- [5] Huang W, Shuk P and Greenblatt M 1997 *Solid State Ionics* **100** 23
- [6] Fang L 2017 *Int. J. Electrochem. Sci.* **12** 218
- [7] Dunyushkina L, Gorbunov V, Babkina A and Esina N 2003 *Ionics* **9** 67
- [8] Gorelov V and Balakireva V 1997 *Electrochemistry* **33** 1450
- [9] Dunyushkina L and Gorbunov V 2001 *Inorg. Mater.* **57** 1165
- [10] George W and Grace R 1969 *J. Phys. Chem. Solids* **30** 881
- [11] Arita Y, Nagarajan K, Ohashi T and Matsui T 1997 *J. Nucl. Mater.* **247** 94
- [12] Dunyushkina L and Gorelov V 2013 *Solid State Ionics* **253** 169
- [13] Ahmed M and Bishay S 2009 *Mater. Chem. Phys.* **114** 446
- [14] McCammon C, Becerro A, Langenhorst F, Angel R, Marion S and Seifert F 2000 *J. Phys. Condens. Matter* **12** 2969
- [15] Cheng J, Bao W, Zhu D and Ding M 2009 *J. Alloys Compd.* **486** 895
- [16] Hreniak D, Strek W, Chmielowiec J, Pasciak G, Pazik R, Gierlotka S and Lojkowski W 2006 *J. Alloys Compd.* **408-412** 637
- [17] Mei A, Jiang Q, Lin Y and Nan C 2009 *J. Alloys Compd.* **486** 871
- [18] Shin K, Ko Y and Shin D 2011 *J. Alloys Compd.* **509S** S478
- [19] Wang H, Cheng J, Zhai L and Cheng 2007 *J Solid State Commun.* **142** 710
- [20] Liang K, Du Y and Nowick A 1994 *Solid State Ionics* **69** 117
- [21] Muccillo R and Carmo J 2012 *Mater. Res. Bull.* **47** 1204
- [22] Wu X, Li X, Zhang Y, Xu M and He Z 2004 *Mater. Lett.* **58** 1227
- [23] Murashkina A, Demina A, Demin A, Maragou V and Tsiakaras P 2008 *Solid State Ionics* **179** 1615
- [24] Vashook V, Vasylechko L, Ullmann H and Guth U 2003 *Solid State Ionics* **158** 317